

MICHAŁ KARCZ^{*}, SEBASTIAN KOWALCZYK, JANUSZ BADUR

ON THE INFLUENCE OF GEOMETRIC MICROSTRUCTURAL PROPERTIES OF POROUS MATERIALS ON THE MODELLING OF A TUBULAR FUEL CELL

Energy Conversion Department, Institute of Fluid Flow Machinery, Polish Academy of Sciences, Gdańsk

A numerical model of tubular solid oxide fuel cell (SOFC) with simplified one-dimensional current flux prediction is examined. The model takes into account geometric properties of porous sinters used for anode and cathode. Three characteristic parameters, i.e. porosity, tortuosity and mean pore radii have been considered. The obtained numerical results allow one to estimate the influence of various geometric properties of porous materials on the fuel cell performance by means of average and local variables.

Przedstawiono wyniki analizy numerycznej modelu rurkowego ogniwa paliwowego uwzględniającego podstawowe mikrostrukturalne parametry geometryczne porowatych elektrod. Rozważano trzy podstawowe parametry geometryczne: porowatość, krętość oraz średni wymiar porów. Uzyskane rezultaty umożliwiają ocenę wpływu poszczególnych wielkości charakteryzujących obszar porowaty na globalne osiągi ogniwa i lokalne wartości temperatury i gęstości prądu.

1. INTRODUCTION

The principle of operation of fuel cells is based on the direct energy conversion from the chemical to the electrical form. It gives a possibility of more efficient power production in the nearest future. The high temperature solid oxide fuel cell (SOFC) is built mainly from nanomaterials. It consists of two porous electrodes separated by a dense solid electrolyte. Finding of a solid-state material that can operate at temperatures as high as 1000 °C is a serious challenge. Porous sinters have recently been developed by a number of SOFC manufacturers [1]. They developed technology that employs several ceramic sinters which allow to oxygen ions O^{2-} conductivity. An electrolyte has been yield from yttria-stabilized zirconia (YSZ). Anode supported fuel cells are usually based on cermets fabricated from nanopowder mixtures, and the cathode is prepared from lanthanum strontium manganite ($LaSrMnO_3$), or others similar perovskite-type ceramic cathode materials [2].

^{*}Corresponding author, e-mail: mkarcz@imp.gda.pl

Solid-oxide fuel cell is a proecological device with steam as a main product. High temperature of operation makes it possible to get hydrogen directly from natural or synthesis gases via an internal reforming [3]. Low pollutants and noise levels make fuel cells environmentally friendly. On the other hand, a high cost of components of fuel cells is a real disadvantage. Then, it is necessary to develop an appropriate mathematical and numerical model of SOFC performance to avoid a massive number of experimental trials. There are a lot of numerous mathematical models in the literature. A comprehensive review of modelling issues of solid oxide fuel cells one can find in several papers by Kee et al. [2], Kakac et al. [4] and Ma et al. [5]. In the present paper, a three-dimensional model for tubular fuel cell is evaluated. Only single phase electrodes have been considered with uniform microstructure along their thickness. Our aim was to analyze a possible influence of various structural parameters on the electrical circuit and temperature field throughout the SOFC. Three main geometric properties of porous materials have been taken into account, namely: porosity factor ε , tortuosity τ and mean pore radii r .

2. MODEL DESCRITPION

Mathematical model used in the present study has been presented elsewhere [6, 7]. Only these parts of the model that are directly related to the microstructural parameters of porous domains have been highlighted.

General principles of fuel cell operation are very well known. The products of overall reaction are steam and free electrons transfer leading to an electric current flow. The current flux can be expressed with formula originating from the classical Ohm law [4, 8]:

$$\vec{i} = -\sigma \text{grad} \phi \quad (1)$$

where conductivity σ is a material property, and symbol ϕ represents the electric field potential. The classical Nernst formulation can help in estimation of theoretical voltage U_0 generated in a fuel cell [2, 4, 9, 10]. The operating voltage U_{cell} is however lower than the theoretical one due to activation, concentration and ohmic polarizations:

$$U = U^0 - \sum \eta(i) = U^0 - [\eta_{\text{act}}(i) + \eta_{\text{ohm}}(i) + \eta_{\text{conc}}(i)] \quad (2)$$

Numerical implementation and validation of the model have been described previously [6, 7]. In this method, the electric current flux is not considered at the same numerical grid as for the main governing equations in CFD formulation. Then the fuel cell tube is additionally discretized into several segments n as shown in Fig. 1, where all parameters employed for local current flux prediction can be assumed as circum-

ferentially uniform. In the present analysis, local changes of electric flux are obtained implicitly from polarizations through Eqs. (2) under assumptions of constant terminal voltage across interconnectors.

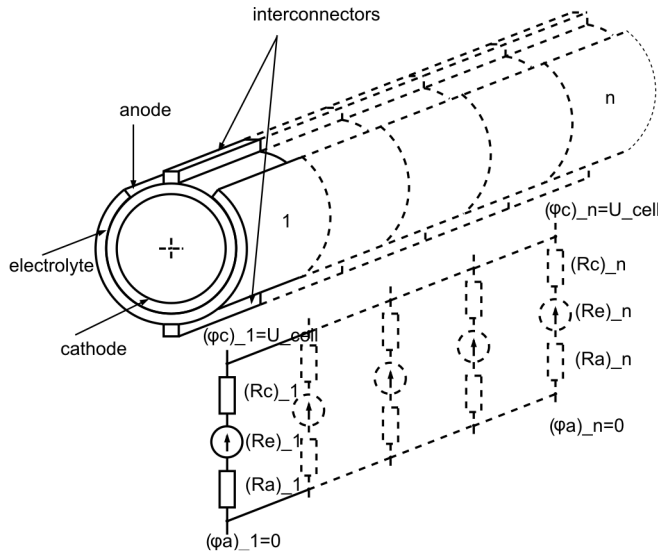


Fig. 1. Tubular fuel cell discretization for 1D electrical field prediction [6, 7]

A mathematical model of SOFC is based on the elementary balance equations solved for fluids: continuity, momentum, energy, and transport of species [11]. Additionally, in order to describe electrochemical equation correctly, the calculations for electric current flux in axial direction have been performed. A general form of mentioned equations is similar to that presented in literature [4, 5, 8, 9]

$$\begin{aligned}
 \frac{\partial}{\partial t} \begin{Bmatrix} \epsilon \rho \\ \epsilon \rho \vec{v} \\ \epsilon \rho e + (1 - \epsilon) \rho_s e_s \\ \epsilon \rho Y_k \\ 0 \end{Bmatrix} + \text{div} \begin{Bmatrix} \epsilon \rho \vec{v} \\ \epsilon \rho \vec{v} \otimes \vec{v} \\ \epsilon \rho e + (1 - \epsilon) \rho_s e_s \\ \epsilon \rho Y_k \\ 0 \end{Bmatrix} + \text{div} \begin{Bmatrix} 0 \\ \epsilon \rho \vec{I} \\ \epsilon \rho \vec{v} \\ 0 \\ 0 \end{Bmatrix} \\
 \text{div} \begin{Bmatrix} 0 \\ \epsilon \vec{\tau} \\ \epsilon \vec{\tau} \vec{v} + \vec{q} \\ \epsilon \vec{J}_k \\ \vec{i} \end{Bmatrix} + \begin{Bmatrix} \epsilon \rho S_m \\ \epsilon \rho S_v \\ \epsilon \rho S_e \\ \epsilon \rho S_k \\ S_\phi \end{Bmatrix}
 \end{aligned} \tag{3}$$

where t – time, ρ – density, \vec{v} – velocity vector, Y_k – mass fraction of species k , e – total energy, p – pressure, ε – porosity factor, \vec{I} – Gibbs' idemfactor, $\vec{\tau}$ – total diffusive momentum flux, \vec{q} – total diffusive heat flux, \vec{J}_k – diffusive flux of species k , S_m – mass source, \vec{S}_v – momentum source, S_e – energy source, S_k – creation/destruction source of species k , and S_ϕ – charge source, subscript s refers to solid.

2.1. CLOSURES USING MICROSTRUCTURAL PARAMETERS

Three characteristic microstructure parameters should be accounted for whenever porous domain is considered, i.e. porosity ε , tortuosity τ and mean radius of pores r [12, 13]. The porosity factor ε is defined as a parameter that indicates the amount of fluid volume V_f in a finite volume V [14]:

$$\varepsilon = \frac{V_f}{V} \quad (4)$$

Tortuosity τ is defined as the ratio of the porous channel length to the straight distance between the end surfaces of the control volume. Tortuosity together with porosity indicates the ratio of the active surface to the volume of electrodes. Mean radius of pores r is another basic geometrical parameter determining the pore dimension. All these parameters are involved mainly in the diffusive transport of species throughout a fuel cell. Three main diffusion mechanisms, i.e. molecular diffusion in gas channels, Knudsen diffusion and Darcy's pressure driven flow can be considered in porous electrodes [2].

The diffusive flux \vec{J}_k can be calculated based on Fick's law with an effective diffusion coefficient D_k^{eff} that accounts an influence of molecular D_k^m and Knudsen diffusion D_k^K according to the formula given by Yakabe et al. [15]:

$$\frac{1}{D_k^{\text{eff}}} = \frac{\tau}{\varepsilon} \left(\frac{1 - \alpha_k x_k}{D_k^m} + \frac{1}{D_k^K} \right) \quad (5)$$

where the coefficient α_k depends on the molecular weight of species. Knudsen diffusivity has the standard form which involves mean pore radius [16]:

$$D_k^K = \frac{2}{3} r \left(\frac{8RT}{\pi M_k} \right)^{1/2} \quad (6)$$

Darcy's pressure-driven force has been included through the source term \vec{S}_v in the momentum equation in the form given in [17, 18]. The permeability of electrodes, i.e.

the parameter for Darcy's force estimation, has been determined by Kozeny–Carman [17, 18]:

$$B = \frac{\varepsilon^2}{72\tau(1-\varepsilon^2)}(2r)^2 \quad (7)$$

Heat exchange between the fuel cell and environment is not considered. Therefore adiabatic conditions at walls of a fuel cell are employed. No radiative heat transfer has been considered in this study. It should be remembered however that radiation leads to the lowering of the tube temperature [7, 17]. For modelling temperature field in porous domains, the effective heat transfer coefficient λ_{eff} should be introduced, for heat diffusive flux prediction, including solid and fluid parts of a control volume:

$$\lambda_{\text{eff}} = \varepsilon\lambda_f + (1-\varepsilon)\lambda_s \quad (8)$$

Activation polarization involved in Eq.(2) is connected with the energy barrier for initialization of electrochemical reactions and can be estimated implicitly from the Butler–Volmer equation, or directly from its sine-hyperbolic approximation [10]:

$$\eta_{\text{act}} = \frac{2RT}{nF} \sinh^{-1} \frac{i}{i_0} \quad (9)$$

Exchange current density i_0 is usually assumed constant but different for cathode and anode. On the other hand, in the present analysis the Arrhenius type formulas have been employed similarly as in [9, 19]. These formulas have been however extended, to account for influence of porosity ε and mean pore radii r on estimation of current density, according to Ni et al. [20]:

$$i_0^q = k_q \left(\frac{1-\varepsilon}{r} \right) \exp \left(-\frac{E_{\text{act}}^q}{RT} \right) \quad (10)$$

where q corresponds to anode (a) and cathode (c), k is the rate constant and E_{act} is the energy of activation. After Zhang et al. [21], the values of anode and cathode activation energies have been assumed $100 \text{ kJ}\cdot\text{mol}^{-1}$ and $120 \text{ kJ}\cdot\text{mol}^{-1}$, respectively.

3. MODEL IMPLEMENTATION

A variety of fuel cell geometric configurations are currently proposed, the majority basing on tubular or planar arrangements. In the present paper, a tubular geometry examined by Siemens and Westinghouse was employed with basic dimensions given elsewhere [6, 9, 17, 19]. The model has been implemented into commercial Fluent solver using user subroutine technique (UDF) [14], and validated [6, 7]. In the present

analysis identical basic properties of electrodes and electrolyte, and also the same inlet and outlet boundary conditions have been assumed.

The porosity ε , tortuosity τ and mean pore size r that govern mass diffusion processes are the main properties of the electrodes. It is not straightforward to assume a proper value of these parameters during modelling. Usually porosity ε of electrodes is in the range 0.2–0.6, tortuosity factor τ varies between 2 and 10, and a typical mean pore r ranges from 0.5 μm to 10.0 μm for various porous bodies [13]. The aim of the present work was to evaluate the influence of various geometric parameters differing in values on the properties of porous domains. Therefore, the calculations have been made for three ranges of parameters:

- varying porosity i.e., $\varepsilon = 0.3; 0.4; 0.5$; constant $\tau = 3$ and $r = 1 \mu\text{m}$,
- varying tortuosity i.e., $\tau = 2; 3; 4$; constant $\varepsilon = 0.5$ and $r = 1 \mu\text{m}$,
- varying mean pore radius, i.e. $r = 0.5; 1; 2 \mu\text{m}$; constant $\varepsilon = 0.5$ and $\tau = 3$.

Mean values for porosity $\varepsilon = 0.5$, tortuosity $\tau = 3$ and mean pore radii $r = 1 \mu\text{m}$ have been taken the same as in previous papers [6, 7]. Range of the parameters has been assumed arbitrarily from the usually employed one.

4. DISCUSSION OF THE RESULTS

For the sake of clarity, the results of numerical analysis concerning mean characteristics of fuel cell are presented independently for every geometric factor in the subsequent sections. However at first, local changes of current density and temperature along the fuel cell tube are shown.

4.1. AXIAL CHANGES OF CURRENT FLUX AND TEMPERATURE

A one-dimensional model used in the present study allows one to compute an axial variation of current density or temperature. In Figure 2, local changes of current density along the fuel cell tube are presented for changing porosity, tortuosity and mean pore radii at $i_{\text{avg}} = 2500 \text{ A/m}^2$. This value has been arbitrarily assumed from the middle range of tubular fuel cell operation. As can be observed, a drop of flux of electric current in axial direction exists. It is consistent with data reported by Li and Suzuki [22] or Campanari and Iora [9] who also noticed a steady decrease of current density in the downstream direction, apart from entrance area of a fuel cell. Lower porosity factors flatten the field of the current density throughout a fuel cell. The maximum of the current density is shifted towards the centre of the tube with decreasing porosity. Tortuosity has rather inconsiderable influence on the distribution of current density along the tube for the assumed average current density. Only at the entrance area the differences between subsequent curves are more pronounced. Changes of mean pore radii have also a weak impact on the current density field at $i_{\text{avg}} = 2500 \text{ A/m}^2$.

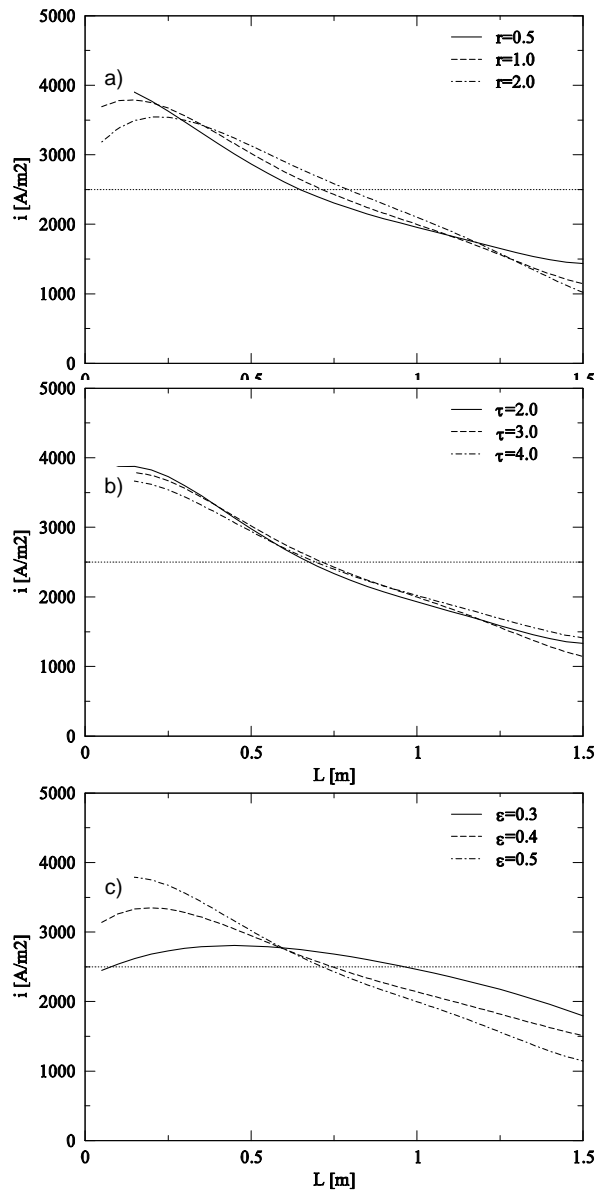


Fig. 2. Distribution of local current flux into the electrolyte along the fuel cell tube for:
 a) changing porosity ϵ , $\tau = 3$ and $r = 1 \mu\text{m}$, b) changing tortuosity τ , $\epsilon = 0.5$ and $r = 1 \mu\text{m}$;
 c) changing mean pore radii r , $\epsilon = 0.5$ and $\tau = 3$

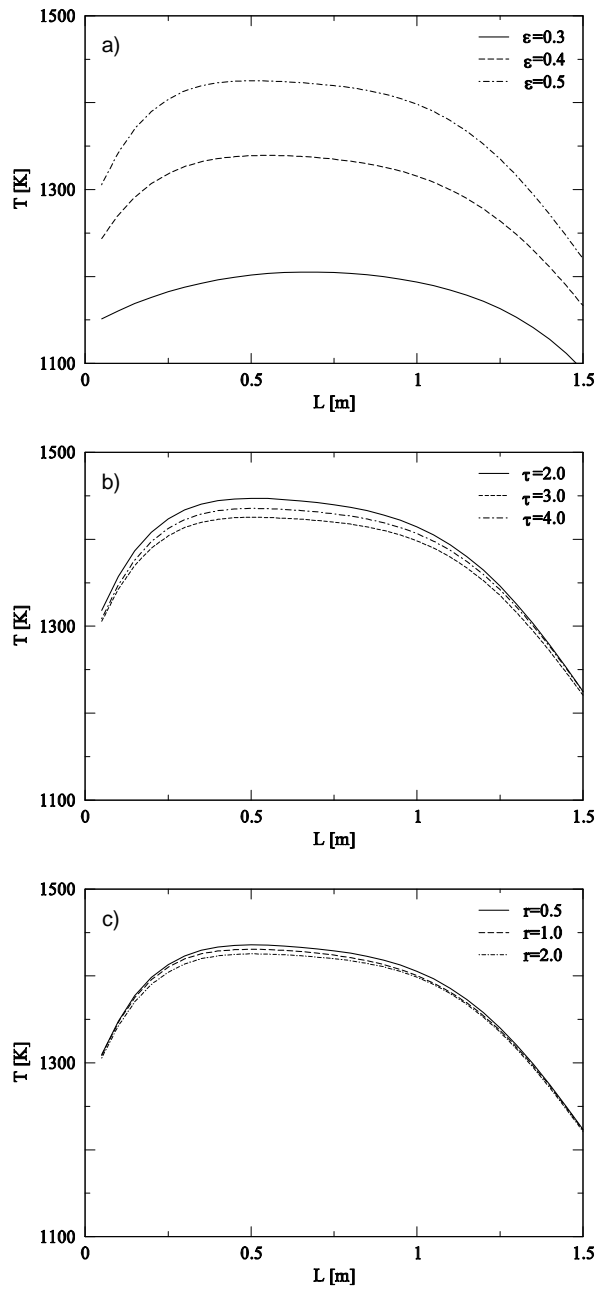


Fig. 3. Distribution of temperature in the electrolyte along the fuel cell tube for:
 a) changing porosity ε , $\tau = 3$ and $r = 1 \mu\text{m}$, b) changing tortuosity τ , $\varepsilon = 0.5$ and $r = 1 \mu\text{m}$,
 c) changing mean pore radii r , $\varepsilon = 0.5$ and $\tau = 3$

The temperature distribution is an important element because it directly influences thermomechanical stresses throughout the fuel cell tube. As can be seen in Fig. 3, the maximum of static temperature is located in the middle of the tube. This observation is similar to the results obtained by other researchers [17, 19, 21]. It is a result of cooling of inlet and exit areas by fresh fuel and air streams, respectively. It should be underlined that porosity factor has a strong impact on the prediction of temperature field. This behaviour can be explained by more efficient cooling due to better heat conductivity when porosity is lower and when increasing influence of a solid part in porous domain can be observed. Changing tortuosity and mean pore radius has only small impact on temperature distribution along the fuel cell tube for the assumed average current density. Generally temperature decreases when tortuosity and mean pore radius increase.

4.2. AVERAGE PERFORMANCE UNDER CHANGES OF POROSITY

The computations have been performed for various average current densities i_{avg} . It allows one to build the characteristics for voltage and power of an operating fuel cell. In Figure 4, dependences of generated voltage on current at various porosities are presented. When lower porosities are assumed, the concentration polarization is higher. On the other hand, for lower current densities, lower porosity makes the fuel cell more efficient due to decreasing activation polarization. Thus voltage diminishes with increasing porosity factor but only for low current densities. At $i_{\text{avg}} = 2500 \text{ A/m}^2$, the generated voltage is almost independent of porosity of electrodes.

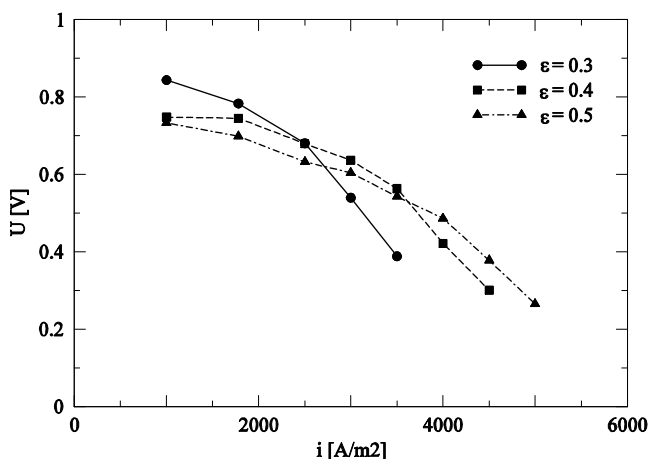


Fig. 4. Voltage–current density characteristics for various porosities

Apparently for higher current densities the voltage increases with increasing porosity. Influence of porosity factor has been also presented by Ni et al. [20] who observed similar trends. Smaller porosity, which means less fluid in the control volume, results in better heat conductivity. Therefore there is also a visible temperature drop due to cooling effect of fresh air and fuel streams with lowering porosity (Fig 2).

Theoretical voltage U_0 based on Gibbs free energy is higher for lower temperature. This is an explanation why generated voltage is also higher for decreasing porosity in the low range of current densities in Fig. 4. On the other hand, when higher average current densities are considered, concentration polarization increases due to arising problem of species transport near reaction zones. For electrodes with lower porosity, where mass diffusion processes are strongly affected, it is even more pronounced. Then, curve for $\varepsilon = 0.3$ in Fig. 4 is more inclined than relevant curve drawn for $\varepsilon = 0.5$. All these issues influence the power generated by a single fuel cell tube.

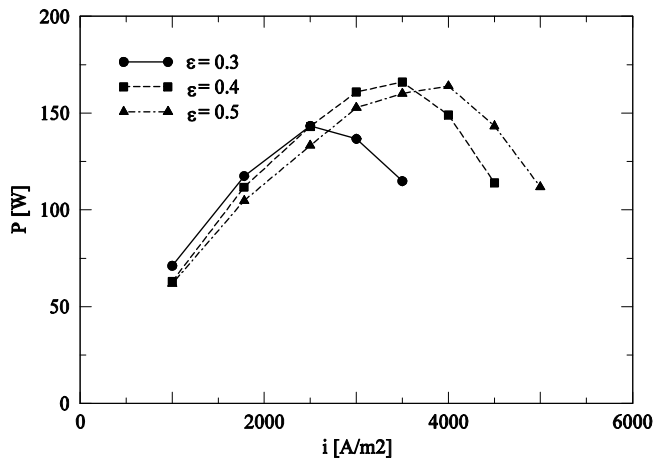


Fig. 5. Power–current density characteristic for various porosities

Decrease in porosity narrows the range of fuel cell operation (Fig. 5). It is direct result of diffusive transport limitation. For increasing porosity, the power maximum shifts towards higher current densities. Porosity factor ε can be replaced by porosity to tortuosity ratio $\psi = \varepsilon/\tau$ [16]. Then for $\varepsilon = 0.3, 0.4, 0.5$ and $\tau = 3$ we have $\psi = 0.100, 0.133, 0.167$, respectively, and the presented results can be directly compared with the data provided by Greene et al. [23] for constant ψ throughout the anode height. However, for such a case we observed partly opposite trend to that presented in [23], where lower values of the ratio ψ were connected with higher generated power for whole range of fuel cell operation. On the other hand, lowering porosity with increasing tortuosity, i.e. lowering value of the ratio ψ , augments concentration polarization and thus limits the range of fuel cell operation. Therefore present results seem to be more consistent.

4.3. AVERAGE PERFORMANCE UNDER VARIATION OF TORTUOSITY

Tortuosity factor τ virtually represents the pore length and its shape [24]. Therefore, a higher tortuosity should explicitly disturb the mass diffusion processes. In comparison to the results presented in Figs. 4 and 5 for various porosity factors, the

impact of tortuosity factor is much smaller, especially for the temperature field. In Figure 6, the voltage–current density characteristics are presented. Increasing tortuosity of porous electrodes lowers fuel cell voltage.

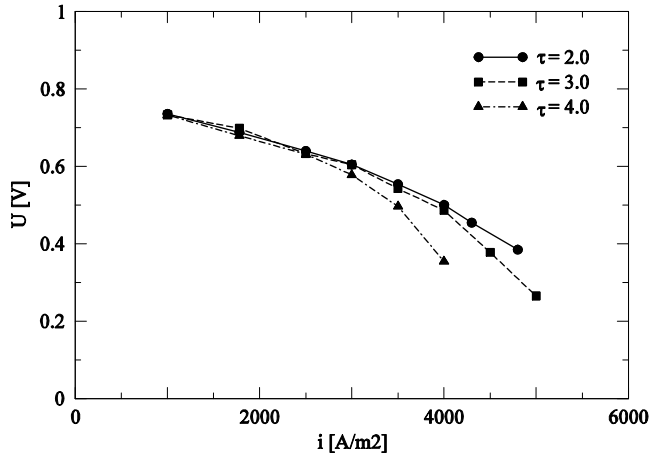


Fig. 6. Voltage–current density characteristics for various tortuosities

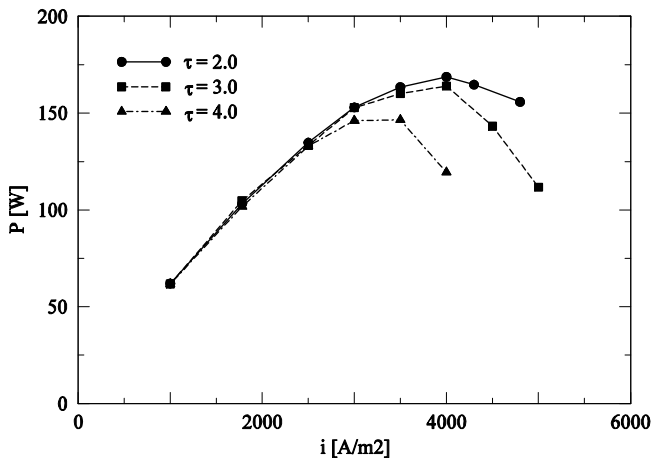


Fig. 7. Power–current density characteristic for various tortuosities

The reasons are similar as for the porosity factor. Increasing gas path to the triple-phase-boundary (TPB) enhances concentration polarization thus affecting the range of fuel cell operation. Power generated by single fuel cell is shown in Fig. 7. In lower range of current densities, $i_{\text{avg}} \leq 2500$ A/m², the power is almost independent of variations of tortuosity. However, at higher current densities increasing tortuosity factor leads to lowering of generated power. There is also a shift of power maximum towards higher i_{avg} with lowering τ . Young and Todd [24] proposed to reinforce the influence

of tortuosity by replacing the ratio of porosity to tortuosity ε/τ usually used in modeling of fuel cells with the ratio ε/τ^2 .

4.4. AVERAGE PERFORMANCE UNDER VARIATION OF MEAN PORE RADII

Mean pore radii have the less prominent influence on the operation of the fuel cell. In Figure 8, the voltage–current characteristics are presented for various mean pore radii.

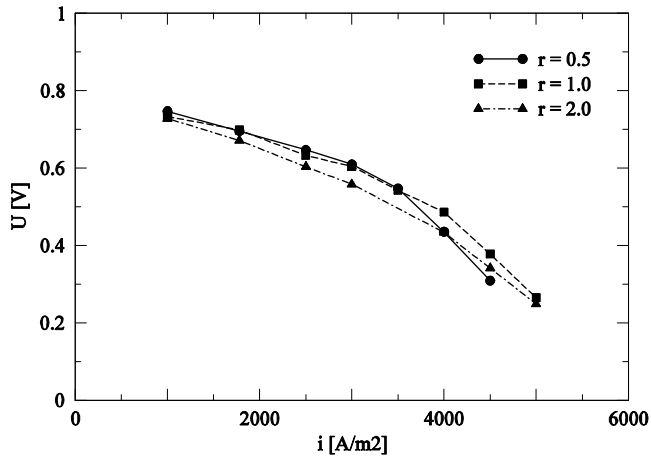


Fig. 8. Voltage–current density characteristic for various mean pore radii

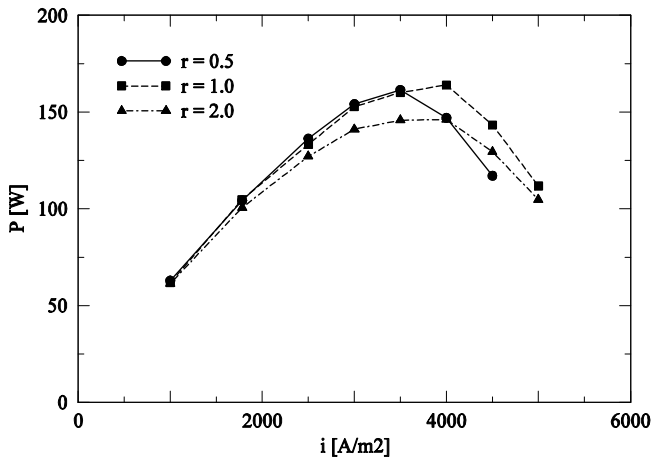


Fig. 9. Voltage–current density characteristic for various mean pore radii

As is clearly visible some differences exist between particular curves for the whole range of fuel cell loading. They are similar to those for changing porosity fac-

tor. Small mean pore radii limit mass diffusion and therefore concentration polarization increases. For smaller mean pore radii, rather a stronger voltage decrease is observed.

The behaviour of power characteristics is quite different as in Fig. 9. Smaller mean pore radii causes narrowing of the fuel cell operation range, but simultaneously the power generated is higher. Maximum power is observed for the current density i_{avg} in the range 3500–4000 A/m² for all considered values of r . Qualitatively similar results are presented by Ni et al. [20] who showed an effect of electrode pore size on the solid oxide fuel cell performance. In their study, the mean pore radius is also employed for estimation of the exchange current density via Eq. (10).

5. CONCLUSIONS

The numerical model dedicated for prediction of performance of solid oxide fuel cells has been described. Variations of microstructural properties of electrodes such as porosity, tortuosity and mean pore radius, and their impact on the fuel cell characteristics, have been numerically investigated. All these parameters are important especially in considerations of diffusive fluxes. However, it was revealed that only porosity factor, that describes fluid to solid volumetric ratio, has a real impact on the fuel cell performance prediction. Porosity strongly affects generated fuel cell voltage mainly through the relevant changes of temperature field due to differences between heat conductivity of fluids and solids. Opposite effects of porosity variation on the activation and concentration polarizations have been numerically confirmed. The tortuosity factor and mean pore radii only slightly affect the temperature field. On the other hand some changes of voltage and power generated by single tubular solid oxide fuel cell can be observed. Therefore assumed model of diffusive transport seems to be quite sensitive to all considered properties.

It is also possible with implemented model to investigate a local changes of current density and temperature under variation of different geometric parameters. Generally lowering porosity flattens current density distribution along the fuel cell and shifts current density maximum towards centre of the fuel cell tube. Lowering mean pore radii influences the current density distribution and shifts its maximum into the fuel cell inlet. On the other hand the tortuosity factor has only a minor impact on the current density distribution. The temperature distribution along the fuel cell tube is affected only via variation of porosity factor. All these observations can help in optimization of geometric structure of porous materials used for electrodes.

ACKNOWLEDGEMENTS

The authors would like to express their gratitude to Dr M. Lemański for his support on this work.

SYMBOLS

B	– permeability, m^2/s
D	– diffusivity coefficient, m^2/s
e	– total energy, J/kg
F	– Faraday constant, C/mol
\vec{T}	– Gibbs' idemfactor
\vec{i}	– electric current flux, A/m^2
j_k	– diffusive flux of mixture component, $kg/m^2 \cdot s$
M	– molecular weight, $kg/kmol$
P	– power, W
p	– pressure, Pa
\vec{q}	– total diffusive heat flux, W/m^2
r	– mean pore radii, m
R	– gas constant, $J/(mol \cdot K)$
T	– temperature, K
t	– time, s
U	– voltage, V
\vec{v}	– velocity vector, m/s
Y	– mass fraction
ε	– porosity factor
ϕ	– electric field potential, V
η	– polarization, V
σ	– electrical conductivity, $1/(\Omega \cdot m)$
ρ	– density, kg/m^3
τ	– tortuosity factor
$\vec{\tau}$	– total diffusive momentum flux, Pa

SUBSCRIPTS AND SUPERSCRIPTS

0	– standard, referential
a	– anode
act	– activation
avg	– average
c	– cathode
conc	– concentration
eff	– effective
k, l	– components of mixture
ohm	– ohmic

REFERENCES

- [1] BOUDGHENE S.A., TRAVERSA E., *Ren. Sust. En. Rev.*, 2002, 6, 433.
- [2] KEE R.J., ZHU H., GOODWIND G., *Solid-oxide fuel cells with hydrocarbon fuels*, Proc. Combustion Institute 2005, 30, 2379.
- [3] BADUR J., LEMAŃSKI M., *Inż. Chem. Proc.*, 2005, 26, 157 (in Polish).
- [4] KAKAC S., PRAMUANJAROENKIJ A., ZHOU X.Y., *J. Hydr. En.*, 2007, 32, 761.
- [5] MA L., INGHAM D.B., POURKASHANIAN M., CARCADEA E., *ASME J. Fuel Cell Sci. Techn.*, 2005, 2, 246.
- [6] KAR CZ M., *Chem. Proc. Eng.*, 2009, 30, 267.

- [7] KARCZ M., *En. Conv. Man.*, 2009, 50, 2307.
- [8] LIN Y., BEALE S.B., *Appl. Math. Model.*, 2006, 30, 1485.
- [9] CAMPANARI S., IORA P.J., *Power Sources*, 2004, 132, 113.
- [10] NOREN D.A., HOFFMAN M.A., *J. Power Sources* 2005, 152, 175.
- [11] BADUR J., *Numerical modeling of sustainable combustion in gas turbines*, Inst. Fluid-Flow Machinery Publ., Gdańsk, 2003 (in Polish).
- [12] CHAN S.H., KHOR K.A., XIA Z.T., *J. Power Sources*, 2001, 93, 130.
- [13] KOWALCZYK S., *Three-dimensional mathematical model of electrochemical reactions in porous sinters of solid oxide fuel cells*, PhD Thesis at the Institute of Fluid Flow Machinery, Polish Academy of Sciences, Gdańsk, 2009 (in Polish).
- [14] *Fluent User Guide*, 2005.
- [15] YAKABE H., HISHINUMA M., URATANI M., MATSUZAKI Y., YASUDA I., *J. Power Sources*, 2000, 86, 423.
- [16] LEHNERT W., MEUSINGER J., THOM F., *J. Power Sources*, 2000, 87, 57.
- [17] SUWANWARANGKUL R., CROISSET E., PRITZKER M.D., FOWLER M.W., DOUGLAS P.L., ENTACHEV E., *J. Power Sources*, 2006, 154, 74.
- [18] ZHU H., KEE R.J., *J. Power Sources*, 2007, 169, 315.
- [19] JIA J., ABUDULA A., WEI L., JIANG R., SHEN S., *J. Power Sources*, 2007, 171, 696.
- [20] NI M., LEUNG D.Y.C., LEUNG M.K.H., *En. Conv. Man.*, 2009, 50, 268.
- [21] ZHANG X., LI G., LI J., FENG Z., *En. Conv. Man.*, 2007, 48, 977.
- [22] LI P.-W., SUZUKI K., *J. Electrochem. Soc.*, 2004, 151, A548.
- [23] GREENE E.S., CHIU W.K.S., MEDEIROS M.G., *J. Power Sources*, 2006, 161, 225.
- [24] YOUNG J.B., TODD B., *Int. J. Heat Mass Transfer*, 2005, 48, 5338.

WPLYW PARAMETRÓW MIKROSTRUKTURALNYCH NA WYNIKI MODELOWANIA RURKOWEGO OGNIWA PALIWOWEGO

Przedstawiono wyniki analizy numerycznej stałotlenkowego ogniwa paliwowego o budowie rurkowej, zasilanego wodorem. Obliczenia wykonano z wykorzystaniem jednowymiarowego modelu wektora gęstości prądu. Zakładano odpowiednie wartości geometrycznych parametrów charakteryzujących porowate spieki, tzn. porowatości, krętości oraz średniej średnicy porów. Parametry te są szczególnie ważne do modelowania dyfuzyjnego strumienia składników reakcji elektrochemicznej, a także dyfuzyjnego strumienia ciepła. Wyniki przedstawiono w postaci zmian lokalnych gęstości prądu i temperatury wzdłuż rurki ogniwa, oraz w postaci globalnych charakterystyk gęstość prądu–napięcie oraz moc–napięcie. Wykazano, że temperatura ogniwa zależy od porowatości elektrod. Wynika to przede wszystkim z różnic między współczynnikiem przewodzenia ciepła w ciele stałym i czynniku gazowym. Mniej porowata elektroda charakteryzuje się większym udziałem ciała stałego w objętości skończonej, co skutkuje lepszym odprowadzaniem ciepła reakcji i w rezultacie niższą temperaturą ogniwa. Napięcie i prąd generowany w ogniwie zależą bezpośrednio od temperatury pracy ogniwa. Zmniejszenie porowatości powoduje wyrównywanie dystrybucji gęstości prądu i przesuwanie jego maksymalnej wartości w kierunku środka rurki ogniwa. Pozostałe parametry geometryczne, tzn. krętość i średnia średnica porów mają ograniczony wpływ na temperaturę ogniwa. Zastosowany model wymiany ciepła w zasadzie nie uwzględnia zmian średniej średnicy porów w rozważanym zakresie średnich gęstości prądu. Parametry te jednak mają istotny wpływ na średnią wartość napięcia i prądu generowanego w ogniwie, głównie przez model dyfuzyjnego strumienia składników reakcji.

Received 23 February 2010